0026-895X/07/7203-665–673$20.00
MOLECULAR PHARMACOLOGY
Copyright © 2007 The American Society for Pharmacology and Experimental Therapeutics
Mol Pharmacol 72:665–673, 2007

Vol. 72, No. 3
34868/3231709
Printed in U.S.A.

Up-Regulation and Increased Activity of $K_V3.4$ Channels and Their Accessory Subunit MinK-Related Peptide 2 Induced by Amyloid Peptide Are Involved in Apoptotic Neuronal Death

A. Pannaccione, F. Boscia, A. Scorziello, A. Adornetto, P. Castaldo, R. Sirabella, M. Taglialatela, G. F. Di Renzo, and L. Annunziato

Division of Pharmacology, Department of Neuroscience, School of Medicine, Federico II University of Naples, Naples, Italy

Received February 7, 2007; accepted May 10, 2007

ABSTRACT

The aim of the present study was to investigate whether $K_V3.4$ channel subunits are involved in neuronal death induced by neurotoxic β-amyloid peptides (Aβ). In particular, to test this hypothesis, three main questions were addressed: 1) whether the Aβ peptide can up-regulate both the transcription/translation and activity of $K_V3.4$ channel subunit and its accessory subunit, MinK-related peptide 2 (MIRP2); 2) whether the increase in $K_V3.4$ expression and activity can be mediated by the nuclear factor-κB (NF-κB) family of transcriptional factors; and 3) whether the specific inhibition of $K_V3.4$ channel subunit reverts the Aβ peptide-induced neurodegeneration in hippocampal neurons and nerve growth factor (NGF)-differentiated PC-12 cells. We found that $A\beta_{1-42}$ treatment induced an increase in $K_V3.4$ and MIRP2 transcripts and proteins, detected by reverse transcription-polymerase chain reaction and Western blot analysis, respectively, in NGF-differentiated PC-12 cells and hippocampal neurons. Patch-clamp experiments performed in whole-cell configuration revealed that the Aβ peptide caused an increase in I_A current amplitude carried by $K_V3.4$ channel subunits, as revealed by their specific blockade with blood depressing substance-I (BDS-I) in both hippocampal neurons and NGF-differentiated PC-12 cells. The inhibition of NF-κB nuclear translocation with the cell membrane-permeable peptide SN-50 prevented the increase in $K_V3.4$ protein and transcript expression. In addition, the SN-50 peptide was able to block $A\beta_{1-42}$-induced increase in $K_V3.4$ K^+ currents and to prevent cell death caused by $A\beta_{1-42}$ exposure. Finally, BDS-I produced a similar neuroprotective effect by inhibiting the increase in $K_V3.4$ expression. As a whole, our data indicate that $K_V3.4$ channels could be a novel target for Alzheimer's disease pharmacological therapy.

Alteration of neuronal K^+ channel function, which is involved in the regulation of membrane excitability—including setting the resting potential, keeping action potentials short, and timing interspike intervals (Birnbaum et al., 2004)—leads to remarkable perturbations in neuronal function. In particular, intracellular potassium concentrations ($[K^+]_i$) play a key role in cell survival. Indeed, a decrease in cytoplasmic $[K^+]_i$, mainly caused by an increased activity of plasma membrane voltage-gated potassium (K_V) channels, triggers cell death (Yu et al., 1997, 1999a,b; Lauritzen et al., 2003), possibly by activating nucleases (Bortner et al., 1997) and caspases (Hughes and Cidlowski, 1999) that, in turn, propagate and amplify death signals. The involvement of K^+ currents in neuronal apoptosis (Yu, 2003) is also supported by the fact that the inhibition of K^+ efflux, induced by a wide range of K^+ channel blockers or by the increase in extracellular K^+ concentration, fully prevents cell death (Pike et al., 1996; Colom et al., 1998). Recent research has demonstrated that changes in K^+ channel activity play a major pathogenetic role in many neurodegenerative disorders, including Alzheimer's disease (AD). In fact, β-amyloid fragments (Aβ),

This study was supported by grants from the Italian Ministry of Health Programma Speciale art. 12bis comma 6, D. Lgs. 229/99; Special Project "Alzheimer 2001/2004" (to L.A. and M.T.), COFIN-MIUR 2002 (to L.A.), COFIN 2004 (to L.A.), PNR-FIRB RBNE01E7YX_007 2001, Regione Campania GEAR, Ricerca Finalizzata Ministero della Salute legge 502/92 "Geni Vulnerabiltà e di Riparazione DNA" (to L.A.), and POP and legge 41 from Regione Campania, 12th Italian-Chinese executive program for scientific and technological cooperation for the period 2006 to 2009 from the Italian Foreign Ministry (to L.A.).

Article, publication date, and citation information can be found at http://molpharm.aspetjournals.org.

doi:10.1124/mol.107.034868.

ABBREVIATIONS: K_V channels, voltage-gated K^+ channels; Aβ, β-amyloid peptide; $A\beta_{1-42}$, β-amyloid peptide 1–42; AD, Alzheimer's disease; BDS-I, blood depressing substance-I; GAPDH, glyceraldehyde 3-phosphate dehydrogenase; I_A, fast inactivating K^+ currents; MIRP, MinK-related peptide; NGF, nerve growth factor; NF-κB, nuclear factor κB; PBS, phosphate-buffered saline; RT-PCR, reverse transcription polymerase chain reaction; ANOVA, analysis of variance; bp, base pair(s); SN-50, NF-κB cell-permeable inhibitory peptide (AAVALLPAVLLALLAPVQRKRQKLMP).

generated upon processing of the integral membrane amyloid precursor protein (Suh and Checler, 2002), alter the properties of K^+ currents in mammalian neurons (Jalonen et al., 1997; Yu et al., 1998; Jhamandas et al., 2001; Ramsden et al., 2001; Pannaccione et al., 2005). Furthermore, a study performed on SN56 cells, a cholinergic cell line from rat, reported that treatment with Aβ increased the amount of delayed rectifier K^+ currents and increased cell death (Colom et al., 1998). Among the different K_V currents exhibiting distinct biophysical properties, fast-inactivating K^+ currents (I_A), which are known to contribute to action potential repolarization (Rudy and McBain, 2001) and to regulate interspike interval, have been suggested to participate in neurodegenerative processes (Birnbaum et al., 2004). The genes encoding for several K_V channel subunits that give rise to I_A currents have been cloned. Among these are K_V4.1, 4.2, and 4.3 of the *Shal* family, K_V3.3 and 3.4 of the *Shaw* family, and K_V1.4 of the *Shaker* subfamily. These channel subunits differ in their pharmacology and biophysical characteristics. In particular, the expression and modulation of the K_V3 subfamily play a relevant role in axons and presynaptic terminal electrophysiological control. In fact, these channels are able to keep action potentials short and to facilitate recovery of processes that accumulate during repetitive action potentials. Furthermore, they can also limit the frequency of action potential transmission. One of the components of K_V3 family, namely K_V3.4, besides being present in skeletal muscle and in sympathetic ganglia (Rudy et al., 1999), is also prominently expressed in the neurons of the adult dentate gyrus and in the mossy fibers of the hippocampus. In these neurons, K_V3.4 subunits seem to be predominantly expressed on axons and nerve terminals (Heinemann et al., 1996; Rudy et al., 1999). Moreover, K_V3.4 subunits can form stable complexes with MinK-related peptide 2 (MIRP2). Such an interaction modifies the voltage-dependence of activation, speeds the recovery from inactivation, reduces the cumulative inactivation, and finally, affects unitary conductance of K_V3.4 channels (Abbott et al., 2001, 2006). In addition, K_V3.4 channel subunits can form heteromeric channels by coassembling with other members of the K_V3 subfamily, such as K_V3.1, K_V3.2, and K_V3.3 channel subunits (Rudy et al., 1999; Rudy and McBain, 2001).

Although it has been demonstrated recently that $A\beta_{1-42}$ can potentiate the I_A (Pannaccione et al., 2005), the molecular identity of K^+ channel subunit(s) modulated by the neurotoxic peptide has not yet been determined. Thus, we investigated whether K_V3.4 channel subunits and its accessory subunit MIRP2 are involved in Aβ-induced I_A modulation. In addition, the hypothesis that the overexpression and hyperactivity of K_V3.4 channels could be related to the apoptotic process induced by Aβ was evaluated by the inhibition of K_V3.4 channel and by the blockade of the nuclear translocation of NF-κB, the transcription factor involved in Aβ neurotoxicity.

The data obtained showed that the Aβ peptide induced an increase in I_A currents through an up-regulation of K_V3.4 channel subunit and MIRP2. Thus, the increase in K_V3.4 functional activity is involved in Aβ neurotoxicity.

Materials and Methods

Materials

β-Amyloid peptide 1–42 ($A\beta_{1-42}$) and all other unmentioned materials were from Sigma Chemical (St. Louis, MO). Primary antibodies against K_V3.4 and K_V3.3 channel subunits and MIRP2 β-subunits, as well as nerve growth factor (NGF 2.5S), tetrodotoxin, and blood depressing substance-I (BDS-I) were from Alomone Labs (Jerusalem, Israel). Primary antibody against caspase-3 and anti-rabbit IgG secondary antibody were purchased from Invitrogen (Carlsbad, CA). SN-50 and Protease Inhibitor Cocktail II were purchased from Calbiochem (San Diego, CA). RPMI 1640 medium, horse serum, fetal bovine serum, and phosphate-buffered saline (PBS) were from Invitrogen. L-Glutamine, fetal calf serum, Earle's balanced salt solution, TRIzol lysis buffer, and SuperScript III were from Invitrogen (Carlsbad, CA). Primers for K_V were from Primm (Milan, Italy). AmpliTaq DNA Polymerase was from Eppendorf (Milan, Italy), and RNAase-free DNAase I was purchased from Stratagene (Milan, Italy). The marker Ladder, 100 bp, was purchased from New England Biolabs (Milan, Italy).

Cell Culture

PC-12 Cells. Rat pheochromocytoma cells (PC-12 cells) were grown as described previously (Pannaccione et al., 2005). Cells were seeded at low density on glass coverslips coated with poly(L-lysine) (50 μg/ml). Differentiation of PC-12 cells was achieved by treatment with NGF 2.5S (50 ng/ml) for 7 to 9 days (Greene and Tischler, 1976).

Rat Hippocampal Neuronal Cultures. Hippocampal neurons were obtained from the brains of 18-day-old Wistar rat embryos (Charles River, Sulzfeld, Germany) as described previously (Scorziello et al., 2001). Cytosine arabinoside at 5 μM was added within 48 h of plating to prevent the growth of non-neuronal cells. In all experiments, neurons were cultured in a humidified atmosphere at 37°C with 5% carbonic anhydrase (CO_2) and used after 8 days of culturing.

Electrophysiology

K^+ currents were recorded from NGF-differentiated PC-12 cells and primary rat hippocampal neurons at 20°–22°C using a commercially available amplifier (Axopatch 200A; Molecular Devices, Sunnyvale, CA), as described previously (Pannaccione et al., 2005). In most experiments, the patch-clamp technique in whole-cell configuration was performed using glass micropipettes of 2.5 to 4 MΩ resistance. Currents were filtered at 5 kHz and digitized using a Digidata 1200 interface (Axon Instruments). Data were acquired and analyzed using the pClamp software (version 6.0.4; Axon Instruments). The pipette solution contained the following: 140 mM KCl, 2 mM $MgCl_2$, 10 mM HEPES, 10 mM glucose, 10 mM EGTA, and 1 mM Mg-ATP adjusted at pH 7.4 with KOH. The extracellular solution contained the following: 150 mM NaCl, 5.4 mM KCl, 3 mM $CaCl_2$, 1 mM $MgCl_2$, and 10 mM HEPES, adjusted at pH 7.4 with NaOH. The extracellular solution for all experiments contained 50 nM tetrodotoxin.

To discriminate K^+ current components having distinct inactivation properties (namely an inactivating component I_A and a delayed-rectifier noninactivating component I_{DR}), appropriate electrophysiological protocols were used. The total outward K^+ current ($I_K = I_A + I_{DR}$) was measured by applying, from a holding potential of −80 mV, depolarizing voltage steps of 250-ms duration ranging from −80 to +40 mV. These were preceded by conditioning pulses at −100 mV lasting for 1.5 s to allow full recovery from I_A inactivation. Then, after conditioning pulses delivered at −40 mV lasting for 1.5 s fully inactivated I_A, I_{DR} was isolated by stepping from −80 to +40 mV for 250 ms. The I_A component was thus obtained by subtracting the isolated I_{DR} component from the total K^+ current. Current amplitudes were measured for I_A and I_{DR} at +40 mV, either at the peak or at the end of the depolarizing pulse, respectively. Possible changes in

cell size occurring upon specific pharmacological treatments were calculated by monitoring the membrane capacitance of each cell, which is directly related to membrane surface area, and by expressing the current amplitude data as current densities (in picoamperes per picofarad). Capacitive currents were elicited by 5-mV depolarizing pulses from −80 mV and acquired at a sampling rate of 50 kHz. The capacitance of the membrane was calculated according to the following equation: $C_m = \tau_c \cdot I_o/\Delta E_m(1 - I_\infty/I_o)$, where C_m is membrane capacitance, τ_c is the time constant of the membrane capacitance, I_o is the maximum capacitance current value, ΔE_m is the amplitude of the voltage step, and I_∞ is the amplitude of the steady-state current.

Assessment of Nuclear Morphology

Nuclear morphology was evaluated by using the fluorescent DNA binding dye bis-Benzimide H 33258 (Hoechst 33258; Aventis, Strasbourg, France). To this aim, cells were fixed in 4% paraformaldehyde and incubated for 5 min in PBS containing 1 μg/ml Hoechst at 37°C. Coverslips were mounted on glass slides and observed with a fluorescence microscopy on a Nikon Eclipse E400 microscope (Nikon, Torrance, CA). Digital images were taken with a CoolSnap camera (Media Cybernetics Inc, Silver Spring, MD), stored on the hard-disk of a Pentium III computer, and analyzed with the Image-Pro Plus 4.5 software (Media Cybernetics Inc). Pathological nuclei were characterized by chromatin condensation (pyknosis), fragmentation, or by a decrease in size.

mRNA Analysis by Reverse-Transcription Polymerase Chain Reaction

Possible changes in RNA expression induced by $A\beta_{1-42}$ treatment were evaluated by semiquantitative RT-PCR. In brief, total RNA was extracted from NGF-differentiated (control) or $A\beta_{1-42}$ treated PC-12 cells using TRIzol lysis buffer (Invitrogen). To avoid contamination by genomic DNA, the extracted RNA was treated with 10 U/μl RNase-free DNAase I for 1 h at 37°C. The purity and integrity of the RNA was checked by denaturing agarose gel electrophoresis. Total RNA (2 μg) was reverse-transcribed by SuperScript III reverse transcriptase (Invitrogen) for 1 h at 50°C using oligo(dt) primers. The retrotranscribed cDNAs were amplified in an MJ Research Minicycler (MJ Reseach PTC 2000 Thermal Cycler; CELBIO, Milano, Italy) by the polymerase chain reaction using primers directed against several cDNAs (Table 1). Primers directed against glyceraldehyde 3-phosphate dehydrogenase (GAPDH) cDNA were used as internal control. The amplification protocol (30 cycles) was the following: 94°C for 30 s, 50°C for 30 s, and 72°C for 1 min. Each 50-μl reaction contained 1.25 U of AmpliTaq DNA Polymerase (Eppendorf) and 10 pmol of each primer. The amplification products were visualized on agarose (2%) gel electrophoresis by loading approximately half (25 μl) of each reaction per lane. The acquisition and densitometric analysis of the RT-PCR products were realized using a ChemiDoc station (Bio-Rad, Milan, Italy).

Western Blot Analysis

Cells were washed in PBS and collected by gentle scraping in ice-cold lysis buffer to detect $K_V3.4$, $K_V3.3$, and MIRP2 proteins (Secondo et al., 2003) or immunoprecipitation assay buffer to detect caspase-3 protein expressions (Amoroso et al., 2002). Both lysis buffers contained Protease Inhibitor Cocktail II (Roche Diagnostics, Monza, Italy). To evaluate $K_V3.4$, $K_V3.3$, and MIRP2 expressions, proteins (100 μg per lane) were separated by SDS-polyacrylamide gel electrophoresis on 8% polyacrylamide gels and transferred onto nitrocellulose membranes (Hybond-ECL; GE Healthcare, Chalfont St. Giles, Buckinghamshire, UK). $K_V3.4$, $K_V3.3$, and MIRP2 expressions were analyzed with anti-$K_V3.4$-, $K_V3.3$-, and MIRP2-polyclonal antibodies. For caspase-3 expression, proteins (50 μg per lane) were separated by SDS-polyacrylamide gel electrophoresis on 12% polyacrylamide gels and transferred onto nitrocellulose membranes (Hybond-ECL; Amersham). Caspase-3 expression was analyzed with anti caspase-3-polyclonal antibody. The chemiluminescence detection was performed by using ECL Western Detection Kit (Amersham). Nonspecific binding sites were blocked by incubation for 2 h at room temperature with 5% nonfat dry milk (Bio-Rad) in Tris-buffered saline/Tween 20 buffer. Films were developed using a standard photographic procedure, and quantitative analysis of detected bands was carried out by densitometer scanning.

$K_V3.4$ Immunofluorescence

NGF-differentiated PC12 cells and hippocampal neurons, both during control condition and after 24 h of $A\beta_{1-42}$ exposure, were washed in cold PBS and fixed in 4% (w/v) paraformaldehyde in PBS for 30 min. After four washes in PBS, the cells were first preincubated in PBS containing 3% (w/v) bovine serum albumin (Sigma) and 0.05% (v/v) Triton X-100 (Bio-Rad) for 30 min and then with the primary anti N-terminal $K_V3.4$ polyclonal antibody (1:2000) at 4°C overnight. Next, cells were washed in PBS and finally incubated with the secondary antibody Alexa-fluor 546 anti-rabbit IgG (Molecular Probes; dilution, 1:200) for 1 h at room temperature. Cell nuclei were stained with Hoechst (Sigma). After the final wash, cells were mounted and placed on coverslips with Vectashield (Vector Laboratories, Burlingame, CA). Slides were analyzed with a Nikon Ecilpse 400 upright microscope (Nikon Instruments, Florence, Italy) equipped with a charge-coupled device digital camera (Coolsnap-Pro) and Image Pro-Plus software (both from Media Cybernetics).

β-Amyloid Peptide Treatment

$A\beta_{1-42}$ was prepared as 0.1 mg/0.1 ml stock solution in sterile PBS, incubated at 37°C for 24 h to enhance aggregation, and stored at −20°C. Stock solution was directly diluted in cell culture media to give the desired experimental concentrations (5 μM).

TABLE 1
mRNA primer sequences

Gene	Primer Sequence	Expected Size
$K_V1.4$		
Sense	tgaggatcatgggaggagt	271 bp
Antisense	tctcttacaactggaaccagc	
$K_V2.1$		
Sense	acaacgagtacttcttcgacc	616 bp
Antisense	ctcttgttggattctgtgagg	
$K_V3.1$		
Sense	acagccacttcgactatga	346 bp
Antisense	ctgagcgccaatctcttg	
$K_V3.2$		
Sense	gggcaagatcgagaacaac	320 bp
Antisense	ggtggcgatcgaagaaga	
$K_V3.3$		
Sense	ggcgacagcggtaagatcgtg	202 bp
Antisense	ggtagtagttgagcacgtaggcga	
$K_V3.4$		
Sense	agacgatgagcgggagttgg	202 bp
Antisense	caggcagaaggtggtaatggag	
$K_V4.2$		
Sense	acccctgatcactcttgtgac	522 bp
Antisense	agagcactctctcctgtattgt	
$K_V4.3$		
Sense	ctccctcagcttccgccagacc	270 bp
Antisense	ctgctgggtgccgcgaagagtc	
MIRP2		
Sense	cagatcgcagagtcagtttctagc	596 bp
Antisense	tcgagatgagttccggagacc	
MIRP1		
Sense	accactttagccaacttg	372 bp
Antisense	tcagggtgacactgtgaacc	
GAPDH		
Sense	ccatggagaaggctgggg	195 bp
Antisense	caaagttgtcatggatgacc	

Statistical Analysis

Statistical comparisons between controls and treated experimental groups were performed by ANOVA followed by Newman test or Student's *t* test. Differences were considered to be statistically significant when p values were <0.05.

Results

Up-Regulation of the Transcripts of $K_V3.4$ Channel Subunits and of Its Accessory Subunit MIRP2 in NGF-Differentiated PC-12 Cells Exposed to $A\beta_{1-42}$ Fragment. RT-PCR performed with specific primers against $K_V1.4$, $K_V3.1$, $K_V3.2$, $K_V3.3$, $K_V3.4$, $K_V4.2$, $K_V4.3$, and their related channel subunits, MIRP1 and MIRP2 (Table 1), showed that $A\beta_{1-42}$ treatment (5 μM for 24 h) induced a selective increase in $K_V3.4$ and MIRP2 mRNA expression but a decrease in $K_V4.2$ (Fig. 1). By contrast, Aβ-treatment did not modify $K_V1.4$, $K_V3.1$, $K_V3.2$, $K_V3.3$, $K_V4.3$, and MIRP1 mRNA (Fig. 1).

Overexpression of $K_V3.4$ Channel and of Its Subunit MIRP2 Induced by $A\beta_{1-42}$ in NGF-Differentiated PC-12 Cells and in Hippocampal Neurons. Immunoblot analysis performed with a $K_V3.4$-specific antibody on protein extracts from NGF-differentiated PC-12 cells and hippocampal neurons revealed two bands, one at 75 kDa and the other at 110 kDa, that seem to correspond to native subunit monomer and to glycosylated subunit monomers (McMahon et al., 2004), respectively (Fig. 2). Densitometric analysis showed that the bands at 75 and 110 kDa were both significantly more intense in hippocampal neurons and NGF-differentiated PC-12 cells treated with $A\beta_{1-42}$ fragment than in the controls (Fig. 2, C and D). In contrast, $A\beta_{1-42}$ treatment failed to modify $K_V3.3$ protein expression in these neurons (Fig. 2, A and B). In addition, $A\beta_{1-42}$ exposure induced an increase in MIRP2 protein expression (Fig. 2).

The $K_V3.4$ Inhibitor BDS-I Prevents $A\beta_{1-42}$ Induced Increase of I_A Currents. Patch-clamp experiments, performed in hippocampal neurons, revealed that $A\beta_{1-42}$ treatment (5 μM for 24 h) caused an increase in I_A current amplitude, previously isolated with the voltage subtraction protocol described under *Materials and Methods* (Fig. 3). I_A currents, obtained upon subtraction of I_{DR} from I_K currents, were blocked by the extracellular application of the K_V3 subfamily inhibitor BDS-I (50 nM) (Diochot et al., 1998; Yeung et al., 2005) (Fig. 3). The percentage of the BDS-I inhibition was higher in $A\beta_{1-42}$-treated hippocampal neurons than in control neurons (Fig. 3D).

$A\beta_{1-42}$-Induced Apoptosis Is Accompanied by an Up-Regulation in $K_V3.4$ Channel Subunits in NGF-Differentiated PC-12 Cells and in Hippocampal Neurons. Immunocytochemical analysis, performed with the selective anti-$K_V3.4$ antibodies, revealed a plasma membrane localization and a punctated staining pattern mostly confined throughout the neuropil of NGF-differentiated PC-12 cells and hippocampal neurons (Figs. 4, A and C,

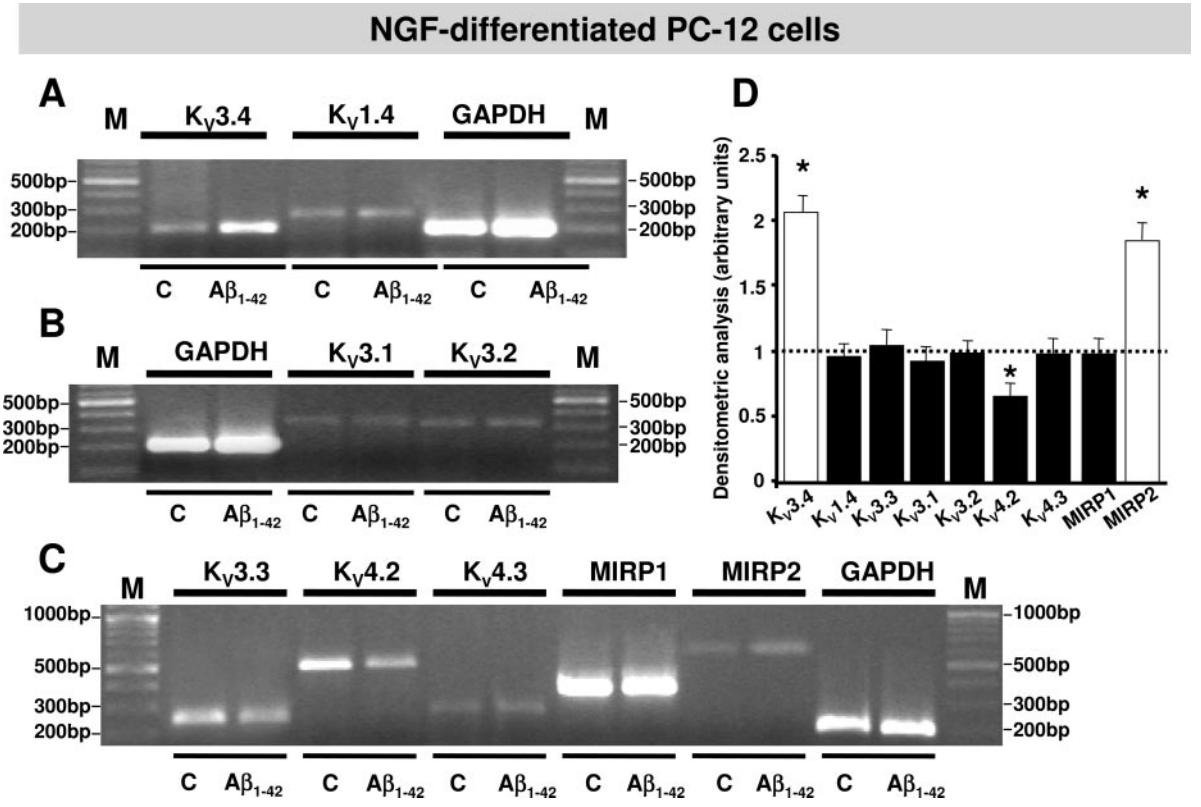

Fig. 1. Up-regulation of the transcripts of $K_V3.4$ channels in NGF-differentiated PC-12 cells exposed to $A\beta_{1-42}$ fragment. A, RT-PCR analysis of $K_V3.4$, $K_V1.4$, and GAPDH mRNA in control and $A\beta_{1-42}$-treated NGF-differentiated PC-12 cells. B, RT-PCR analysis of $K_V3.1$, $K_V3.2$, and GAPDH mRNA in control and $A\beta_{1-42}$-treated NGF-differentiated PC-12 cells. C, RT-PCR analysis of $K_V3.3$, $K_V4.2$, $K_V4.3$, MIRP1, MIRP2, and GAPDH mRNA in control and $A\beta_{1-42}$-treated NGF-differentiated PC-12 cells. GADPH mRNA was used as an internal control to normalize the values. D, densitometric analysis of the ratios between the intensity of the $K_V1.4$, $K_V3.1$, $K_V3.2$, $K_V3.3$, $K_V3.4$, $K_V4.2$, $K_V4.3$, MIRP1, and MIRP2 immunoreactive bands and that of the band corresponding to GAPDH (used as internal control). Data are expressed as mean (±S.E.) values obtained in three separate experiments for NGF-differentiated PC-12 cells and NGF-differentiated PC-12 cells treated with $A\beta_{1-42}$.

and 5A). Similarly to what was observed in Western blot analysis, $A\beta_{1-42}$ exposure increased $K_V3.4$ immunoreactivity signal (Figs. 4, D, F, and G, and 5, B and C). It is interesting that the anti-$K_V3.4$ antibody revealed a pronounced perikaryal staining that was intensely confined to the somatic plasma membrane (Figs. 4, D, F, and G, and 5, B and C). In addition, double-labeling experiments of $K_V3.4$ channel subunits with the fluorescent-DNA binding dye Hoechst 33258 revealed that cells showing $K_V3.4$ channels immunoreactivity after amyloid peptide exposure also displayed an abnormal nuclear morphology (Figs. 4, B and E, and 5, A-a and C-c), thus suggesting that neurons over-

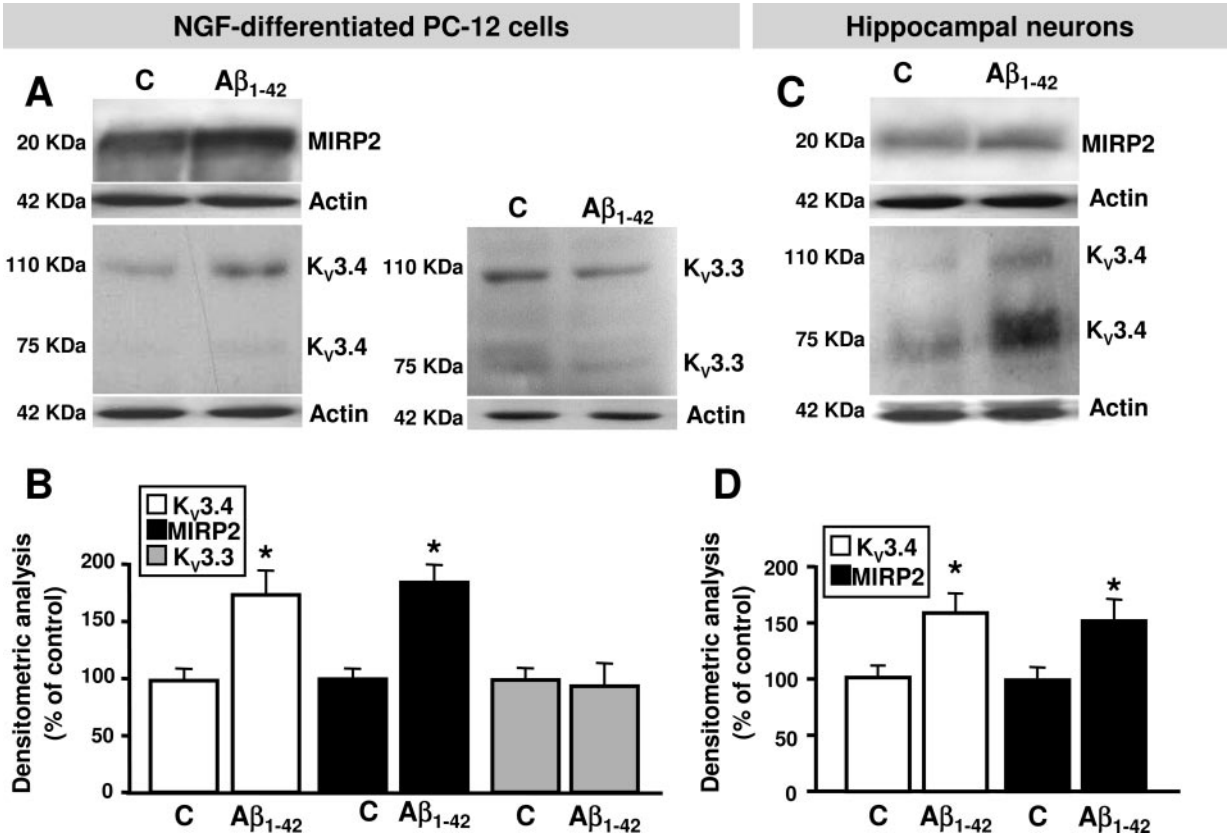

Fig. 2. Overexpression of $K_V3.4$ channels in NGF-differentiated PC-12 cells and in hippocampal neurons induced by $A\beta_{1-42}$. A, effect of $A\beta_{1-42}$ on $K_V3.4$, $K_V3.3$, and MIRP2 protein expression in NGF-treated PC-12 cell. B, densitometric analysis of each experimental group, normalized for the corresponding actin value (used as internal control), is expressed as a percentage of controls. Data are expressed as percentage (±S.E.) values obtained in three separate experiments for NGF-differentiated PC-12 cells and NGF-differentiated PC-12 cells treated with $A\beta_{1-42}$. C, effect of $A\beta_{1-42}$ on $K_V3.4$ and MIRP2 protein expression in hippocampal neurons. D, densitometric analysis of each experimental group, normalized for the corresponding actin value (used as internal control), is expressed as a percentage of controls. Data are expressed as percentage (±S.E.) values obtained in three separate experiments in hippocampal neurons.*, $p < 0.05$ versus control values (Student's t test).

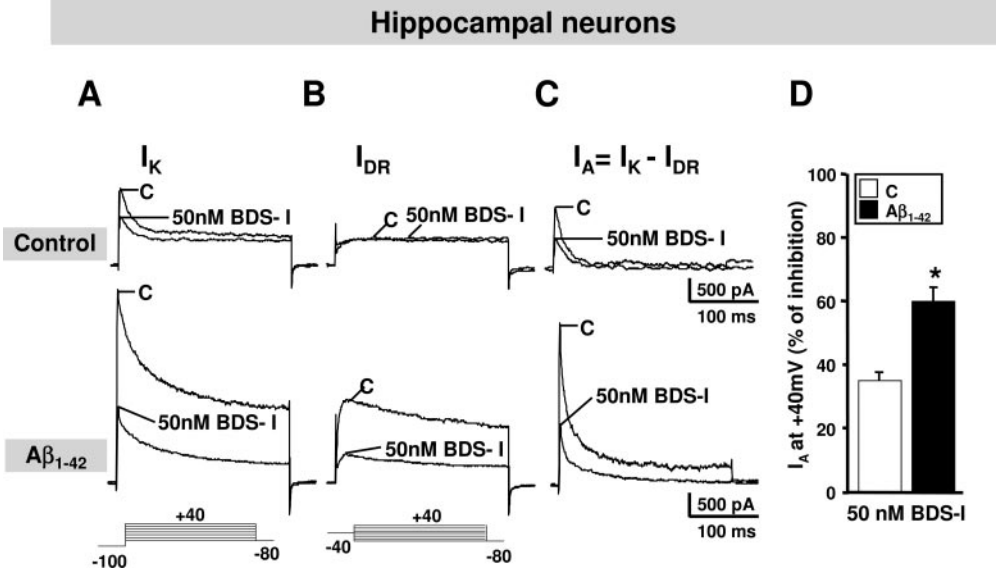

Fig. 3. The $K_V3.4$ inhibitor BDS-I prevents $A\beta_{1-42}$-induced increase of I_A currents. A, total outward K^+ currents recorded from hippocampal neurons exposed to vehicle or 50 nM BDS-I for 5 min (top) or to $A\beta_{1-42}$ (24 h) and $A\beta_{1-42}$+BDS-I (bottom). B, I_{DR} currents recorded from hippocampal neurons exposed to vehicle or 50 nM BDS-I for 5 min (top) or to $A\beta_{1-42}$ (24 h) and $A\beta_{1-42}$+BDS-I (bottom). C, I_A currents obtained in each cell upon subtraction of I_{DR} from I_K currents. D, I_A current quantification expressed as a percentage of inhibition compared with control in the absence or presence of $A\beta_{1-42}$ in hippocampal neurons exposed to 50 nM BDS-I. The values are expressed as mean (±S.E.M.) of current densities recorded from 6 to 40 cells in each experimental group, as indicated. *, $p < 0.05$ versus control values (Student's t test).

expressing this K^+ channel undergo apoptosis. This result was confirmed by Western blot analysis performed with a caspase-3-specific antibody on protein extracts from NGF-differentiated PC-12 cells. In fact, $A\beta_{1-42}$ exposure induced an increase of caspase-3 expression (Fig. 4H). Likewise, 24-h $A\beta_{1-42}$ exposure induced the activation of caspase-3 in hippocampal neurons (Fig. 5D).

Prevention of $A\beta_{1-42}$-Induced Apoptosis by BDS-I in NGF-Differentiated PC-12 Cells and in Hippocampal Neurons. BDS-I (50 nM), the K_V3 subfamily inhibitor, was able to significantly prevent the abnormal nuclear morphology induced by the exposure of NGF-differentiated PC-12 cells (Fig. 6, A and B) and of hippocampal neurons (Fig. 6, C and D) to $A\beta_{1-42}$ (5 μM for 24 h), as detected by the Hoechst 32258 dye staining.

Prevention of Protein and Transcript Expression of $K_V3.4$ Channel Subunits and of Apoptotic Nuclear Features by the Inhibition of NF-κB Nuclear Translocation in NGF-Differentiated PC-12 Cells. RT-PCR (Fig. 7, A and B) and Western blot analysis (Fig. 7, C and D) performed in the presence and in the absence of SN-50 (5 μM)—a cell membrane-permeable peptide capable of inhibiting the nuclear translocation of NF-κB complexes (Lin et al., 1995)—showed that this agent largely prevented the increase in $K_V3.4$ mRNA and protein expression, respectively, caused by $A\beta_{1-42}$ exposure (5 μM, 24 h). Furthermore

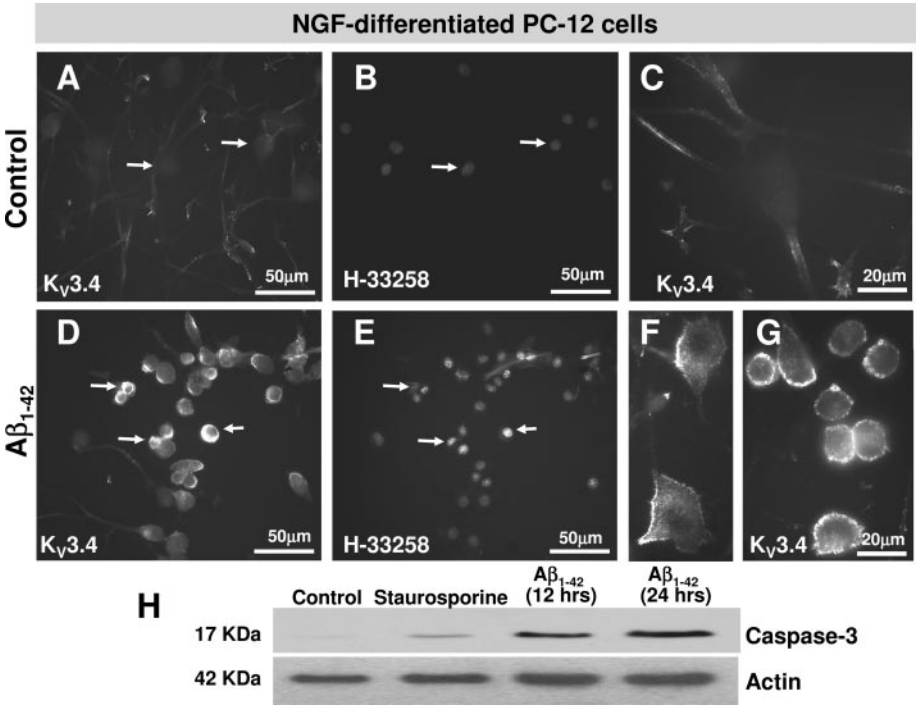

Fig. 4. Effect of $A\beta_{1-42}$ on the distribution of $K_V3.4$ channel subunits and on the apoptotic process in NGF-differentiated PC-12 cells. Double immunofluorescence images of NGF-differentiated PC-12 cells displaying both $K_V3.4$ protein expression and Hoechst-33258 staining in control (A and B, respectively) and in cells exposed to $A\beta_{1-42}$ for 24 h (D and E, respectively). Arrows point to normal (B) or abnormal nuclei (E) showing pyknosis, fragmentation, or a decreased nuclear size. High-magnification images of representative $K_V3.4$ staining pattern in control (C) and $A\beta_{1-42}$-treated NGF-differentiated PC-12 cell (F and G). Arrows point to the $K_V3.4$ immunoreactivity signal along cellular processes of control cells (A and C) or around the soma plasma membrane in $A\beta_{1-42}$-exposed cells (D, F, and G). H, effect of $A\beta_{1-42}$ on caspase-3 expression in NGF-differentiated PC-12 cells. Staurosporine was used as positive control. Scale bar, 50 μm in A, B, D, and E; 20 μm in C, F, and G.

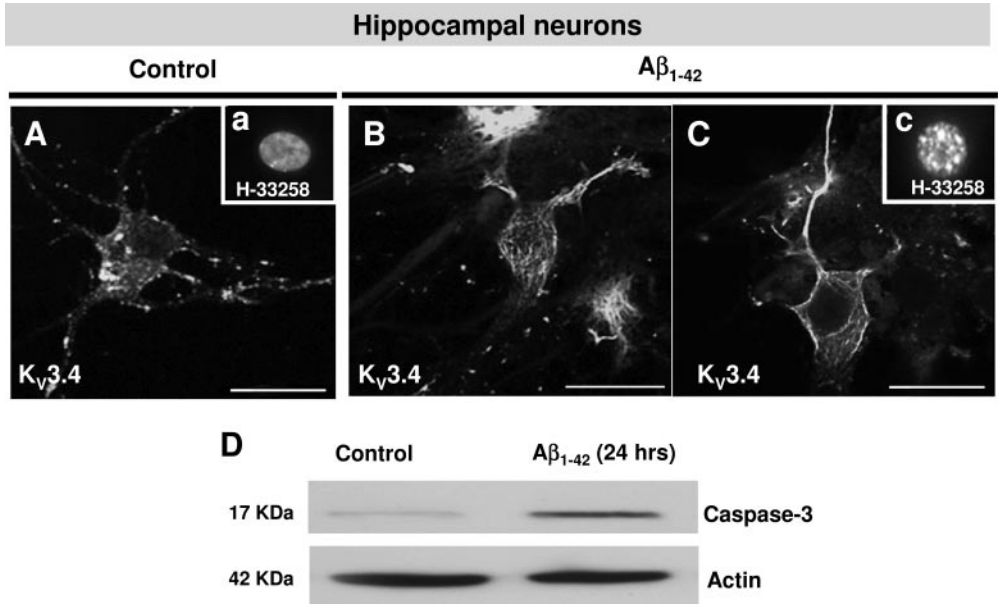

Fig. 5. Effect of $A\beta_{1-42}$ on the distribution of $K_V3.4$ channel subunits and on the apoptotic process in hippocampal neurons. Confocal double immunofluorescence images of a single representative hippocampal neuron displaying both $K_V3.4$ protein expression and nuclear staining in control (A and a, respectively) and in cells exposed to $A\beta_{1-42}$ for 24 h (B–C and c, respectively). B and C refer to the same cell registered with differing focus points. Note the finely punctated $K_V3.4$ labeling in control cells (A, arrows) or the intense perikaryal $K_V3.4$ immunoreactivity in $A\beta_{1-42}$-exposed cells (C, arrows). D, effect of $A\beta_{1-42}$ on caspase-3 expression in hippocampal neuron. Scale bar, 20 μm in A, B, and C.

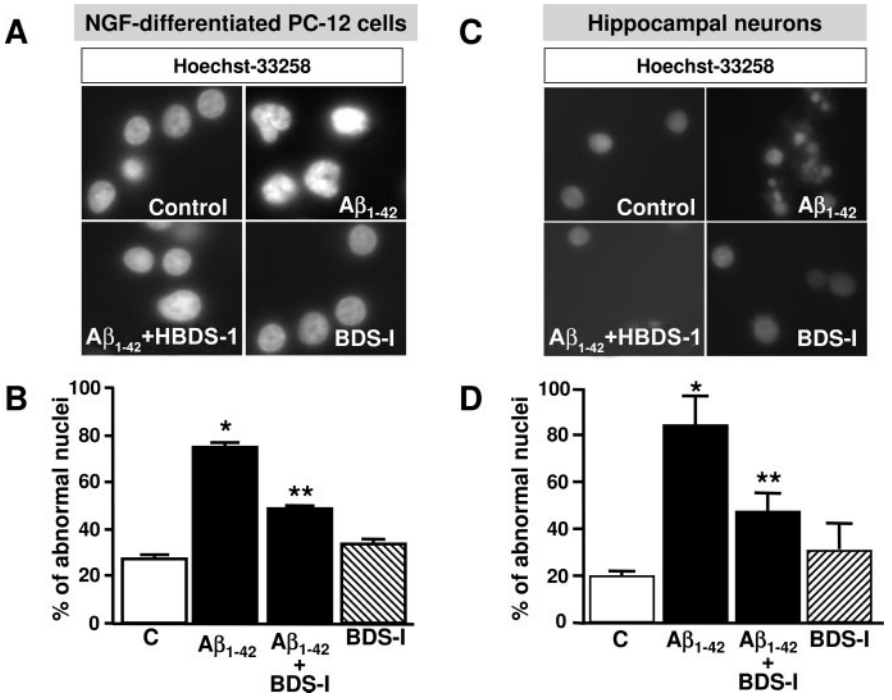

Fig. 6. Prevention of $A\beta_{1-42}$-induced apoptosis by the inhibition of $K_V3.4$ channel activity in NGF-differentiated PC-12 cells and in hippocampal neurons. A, assessment of nuclear morphology with Hoechst-33258 in NGF-differentiated PC-12 cells exposed for 24 h either to 5 μM $A\beta_{1-42}$, to $A\beta_{1-42}$+BDS-I, or to only BDS-I. B, quantification of the results obtained in four separate experiments in which at least 10 microscopic fields were analyzed (approximately 1000 cells per group). *, $p < 0.05$ versus controls; **, $p < 0.05$ versus $A\beta_{1-42}$ groups (Student's and ANOVA test). C, assessment of nuclear morphology evaluated with Hoechst 33258 in primary rat hippocampal neurons in different experimental conditions. D, nuclear morphology quantification assessment with Hoechst 33258 in primary rat hippocampal neurons in different experimental conditions. The mean (±S.E.) values were obtained in four separate experiments in which at least 10 microscopic fields were analyzed (approximately 1000 cells per group). *, $p < 0.05$ versus control groups **, $p < 0.05$ versus $A\beta_{1-42}$ groups (Student's t test and ANOVA).

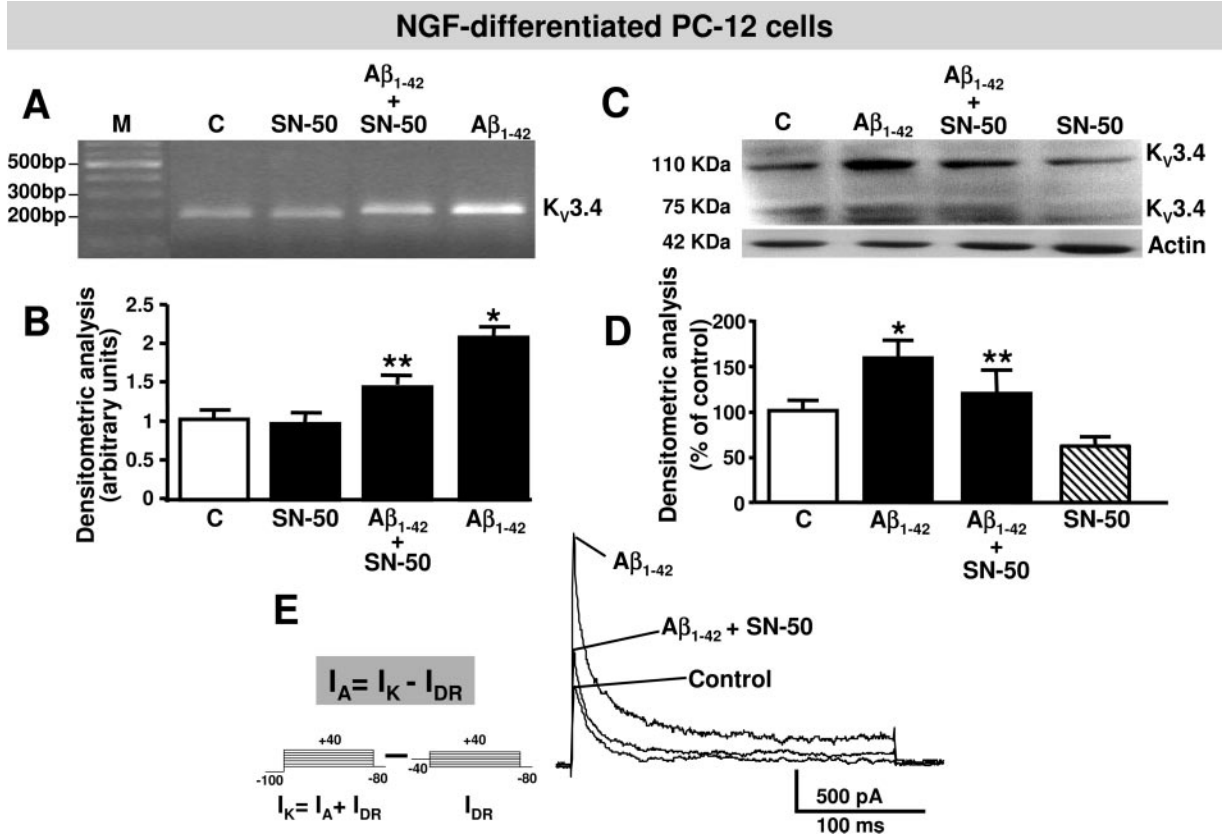

Fig. 7. The inhibition of NF-κB nuclear translocation prevents protein and transcript expression of $K_V3.4$ channel subunits and apoptotic nuclear feature. RT-PCR analysis of $K_V3.4$ in NGF-differentiated PC-12 cells in basal conditions (control group) or exposed for 24 h to either 5 μM $A\beta_{1-42}$, $A\beta_{1-42}$ + SN-50, or SN-50 alone. B, densitometric analysis of the ratios between the intensity of the $K_V3.4$ in the same experimental conditions. Data are expressed as mean (±S.E.) values obtained in three separate experiments in NGF-differentiated PC-12 cells or in cells treated with $A\beta_{1-42}$ in the presence or absence of SN-50, respectively, or in cells exposed only to SN-50. C, effect on $K_V3.4$ protein expression in NGF-treated PC-12 cells under the same experimental conditions. D, densitometric analysis of each experimental group, normalized for the corresponding actin value (used as internal control), is expressed as a percentage of controls. Data are expressed as the percentage mean (±S.E.) values obtained in three separate experiments in NGF-differentiated PC-12 cells or in cells treated with $A\beta_{1-42}$ in the presence or absence of SN-50, respectively, or in cells exposed only to SN-50. E, I_A superimposed traces recorded from NGF-differentiated PC-12 cells untreated and/or exposed for 24 h to 5 μM $A\beta_{1-42}$ in the presence or absence of SN-50, respectively. *, $p < 0.05$ versus control groups; **, $p < 0.05$ versus $A\beta_{1-42}$ groups (Student's t test and ANOVA).

SN-50, the NF-κB inhibitor, was able to prevent $A\beta_{1-42}$-induced increase of I_A current (Fig. 7E).

Discussion

In this study, we provide evidence that hippocampal neurons and NGF-differentiated PC-12 cells exposed to $A\beta_{1-42}$ treatment display a selective up-regulation of $K_V3.4$ channel subunits through the activation of the transcriptional factor NF-κB. In addition, this transcriptional event is associated with a current increase carried by this channel. It is interesting that the action of $A\beta_{1-42}$ was not limited to the pore-forming $K_V3.4$ subunit. Indeed, it also induced an overexpression of MIRP2, a neuronal β-subunit coassembling with $K_V3.4$ subunit and playing a crucial role in the control of its biophysical properties and pharmacological profile (Abbott et al., 2001, 2006). Such MIRP2 overexpression might profoundly interfere with the function of pore-forming $K_V3.4$ α-subunits, suggesting that the neurotoxic Aβ peptide might influence the I_A current by modulating simultaneously the pore-forming α-subunit and its accessory component expression.

On the other hand, $A\beta_{1-42}$ exposure selectively modulated the expression and the activity of $K_V3.4$ channel subunits because the amyloid peptide did not modify the mRNA expression of the other K_V channels, $K_V1.4$, $K_V3.1$, $K_V3.2$, $K_V3.3$, and $K_V4.3$ subunits. In agreement with biochemical and electrophysiological results, the immunocytochemical analysis confirmed that the $A\beta_{1-42}$-induced up-regulation of $K_V3.4$ channel subunit was associated with an altered subcellular distribution of this protein. In fact, $A\beta_{1-42}$ treatment induced a more intense staining for $K_V3.4$ subunits; after $A\beta_{1-42}$ treatment, $K_V3.4$ immunoreactivity was mainly confined to the somatic plasma membrane, compared with that of control cells in which the fluorescent signal was mostly distributed through the neuropil. This different $K_V3.4$ distribution induced by the neurotoxic peptide could be caused by the altered integrity of the cytoskeletal network prompted by oligomeric or fibrillar forms of Aβ (Michaelis et al., 2005). These findings are in accordance with other experiments carried out with rhodaminate-phalloidin, a selective actin fluorescence staining, which revealed that $A\beta_{1-42}$ causes a cytoskeletal rearrangement (Pannaccione et al., 2005). In addition, hippocampal neurons and NGF-differentiated PC-12 cells expressing increased $K_V3.4$ immunoreactivity showed an apoptotic nuclear process, as revealed by caspase-3 activation (Amoroso et al., 2002; Tamagno et al., 2006) and by Hoechst 33258-monitored abnormal nuclear morphology, thus suggesting a possible link between the enhanced expression and function of this K^+ channel and the neurotoxic consequences prompted by Aβ exposure. That the exposure to Aβ fragments may alter the properties of K^+ currents in mammalian neurons (Jalonen et al., 1997; Colom et al., 1998; Yu et al., 1998; Jhamandas et al., 2001; Ramsden et al., 2001; Pannaccione et al., 2005) and therefore may cause an increase in cell death as a result of a decrease in cytoplasmic K^+ concentrations (Bortner et al., 1997; Hughes and Cidlowski, 1999) has already been reported. Nevertheless, the molecular identification of the K^+ channel involved has been a matter of debate. In particular, Pan et al. (2004) showed that a single intracerebroventricular injection of $A\beta_{25-35}$ in rat up-regulates $K_V1.4$ and $K_V2.1$ expression in the hippocampus and $K_V4.2$ in the cortex. Likewise, an up-regulation of $K_V4.2$ channel subunit, carrying I_A current, has also been observed in rat cerebellar granule cells exposed to neurotoxic Aβ peptides (Plant et al., 2006). By contrast, in the present study, the expression of $K_V4.2$ mRNA was down-regulated by neurotoxic $A\beta_{1-42}$. It is noteworthy that the expression of $K_V4.2$ gene can be differentially regulated in different cell types or by following several injury models (Tsaur et al., 1992; Jia and Takimoto, 2003).

The hypothesis that $K_V3.4$ channels are involved in the $A\beta_{1-42}$ neurotoxic effect was further supported by the results showing that BDS-I, a $K_V3.4$ blocker (Diochot et al., 1998), exerted a potent neuroprotective action in hippocampal neurons and NGF-differentiated PC-12 cells exposed to $A\beta_{1-42}$ peptide. On the other hand, the possibility that the neuroprotective action of BDS-I is also caused by a blockade of the other HK_V3 subfamily members $K_V3.1$, $K_V3.2$, and $K_V3.3$ (Yeung et al., 2005) does not seem a likely explanation because their expression is unmodified after Aβ peptide exposure.

Regarding the NF-κB family of transcriptional factors, their involvement in AD pathogenesis has long been corroborated by insightful evidence. In fact, an increased NF-κB activity has been detected in neurons and astrocytes in the immediate vicinity of amyloid plaques in brain sections from patients with AD (Ferrer et al., 1998); furthermore, a significant NF-κB activation in primary neuronal cells exposed to Aβ peptides has also been documented (Barger and Mattson, 1996). In addition, data obtained previously in our laboratory (Pannaccione et al., 2005) have revealed that the highly specific and cell membrane-permeable NF-κB inhibitor SN-50 (Lin et al., 1995) exerts a significant neuroprotective effect upon $A\beta_{1-42}$ exposure (Pannaccione et al., 2005). In the present study, SN-50 largely prevented the increase in $K_V3.4$ protein expression and activity triggered by $A\beta_{1-42}$ exposure, suggesting that NF-κB mediates the transcriptional regulation of $K_V3.4$ occurring during Aβ exposure. Further evidence that the increased expression of $K_V3.4$ channels was caused by the stimulation of protein transcription and synthesis rather than by an inhibition of its catabolism is that $K_V3.4$ mRNA also increased. In addition, other experiments have revealed that the protein synthesis inhibitor cycloheximide and the transcriptional inhibitor actinomycin D fully prevent Aβ-induced K^+ currents (Pannaccione et al., 2005). It is interesting that cDNA array analysis has also demonstrated that the $K_V3.4$ gene is up-regulated in the brain extracts of transgenic mice with the amyloid precursor protein 695 Swedish mutation and in the cerebral cortex of patients in the early and later stages of AD (Angulo et al., 2004).

As a whole, our data suggest that $A\beta_{1-42}$ fragment exposure causes the up-regulation not only of $K_V3.4$ but also of its accessory subunit MIRP2. This increased expression is associated with an enhanced activity of the K^+ current carried by this channel. Furthermore, the changes resulting from this channel activation may contribute to a reduction in $[K^+]_i$, which in turn triggers the apoptotic process, as already demonstrated (Yu, 2003).

In conclusion, the relationship between $K_V3.4$ and apoptotic cell death is demonstrated in the current study by the fact that the blockade of this channel was able to prevent the apoptotic process triggered by $A\beta_{1-42}$ fragment. These results reveal new

and additional therapeutic strategies for AD using selective voltage-dependent potassium channels as molecular targets.

Acknowledgments

We thank Vincenzo Grillo for technical help with animal housing and Dr. Paola Merolla for editorial revision.

References

Abbott GW, Butler MH, Bendahhou S, Dalakas MC, Ptacek LJ, and Goldstein SA (2001) MiRP2 forms potassium channels in skeletal muscle with Kv3.4 and is associated with periodic paralysis. *Cell* **104:**217–231.

Abbott GW, Butler MH, and Goldstein SA (2006) Phosphorylation and protonation of neighboring MiRP2 sites: function and pathophysiology of MiRP2-Kv3.4 potassium channels in periodic paralysis. *FASEB J* **20:**293–301.

Amoroso S, D'Alessio A, Sirabella R, Di Renzo G, and Annunziato L (2002) Ca^{2+}-independent caspase-3 but not Ca^{2+}-dependent caspase-2 activation induced by oxidative stress leads to SH-SY5Y human neuroblastoma cell apoptosis. *J Neurosci Res* **68:**454–562.

Angulo E, Noe V, Casado V, Mallol J, Gomez-Isla T, Lluis C, Ferrer I, Ciudad CJ, and Franco R (2004) Up-regulation of the Kv3.4 potassium channel subunit in early stages of Alzheimer's disease. *J Neurochem* **91:**547–557.

Barger SW and Mattson MP (1996) Induction of neuroprotective kB-dependent transcription by secreted forms of the Alzheimer's β-amyloid precursor. *Brain Res Mol Brain Res* **40:**116–126.

Birnbaum SG, Varga AW, Yuan LL, Anderson AE, Sweatt JD, and Schrader LA (2004) Structure and function of Kv4-family transient potassium channels. *Physiol Rev* **84:**803–833.

Bortner CD, Hughes FM, and Cidlowski JA Jr (1997) A primary role for K^+ and Na^+ efflux in the activation of apoptosis. *J Biol Chem* **272:**32436–32442.

Colom LV, Diaz ME, Beers DR, Neely A, Xie WJ, and Appel SH (1998) Role of potassium channels in amyloid-induced cell death. *J Neurochem* **70:**1925–1934.

Diochot S, Schweitz H, Beress L, and Lazdunski M (1998) Sea anemone peptides with a specific blocking activity against the fast inactivating potassium channel Kv3.4. *J Biol Chem* **273:**6744–6749.

Ferrer I, Marti E, Lopez E, and Tortosa A (1998) NF-kB immunoreactivity is observed in association with βA4 diffuse plaques in patients with Alzheimer's disease. *Neuropathol Appl Neurobiol* **24:**271–277.

Greene LA and Tischler AS (1976) Establishment of a noradrenergic clonal line of rat adrenal pheochromocytoma cells which respond to nerve growth factor. *Proc Natl Acad Sci U S A* **73:**2424–2428.

Heinemann SH, Rettig J, Graack HR, and Pongs O (1996) Functional characterization of Kv channel beta-subunits from rat brain. *J Physiol* **493 (Pt 3):**625–633.

Hughes FM Jr and Cidlowski JA (1999) Potassium is a critical regulator of apoptotic enzymes in vitro and in vivo. *Adv Enzyme Regul* **39:**157–171.

Jalonen TO, Charniga CJ, and Wielt DB (1997) beta-Amyloid peptide-induced morphological changes coincide with increased K^+ and Cl^- channel activity in rat cortical astrocytes. *Brain Res* **746:**85–97.

Jhamandas JH, Cho C, Jassar B, Harris K, MacTavish D, and Easaw J (2001) Cellular mechanisms for amyloid beta-protein activation of rat cholinergic basal forebrain neurons. *J Neurophysiol* **86:**1312–1320.

Jia Y and Takimoto K (2003) GATA and FOG2 transcription factors differentially regulate the promoter for Kv4.2 K^+ channel gene in cardiac myocytes and PC12 cells. *Cardiovasc Res* **60:**278–287.

Lauritzen I, Zanzouri M, Honore E, Duprat F, Ehrengruber MU, Lazdunski M, and Patel AJ (2003) K^+-dependent cerebellar granule neuron apoptosis. Role of task leak K^+ channels. *J Biol Chem* **278:**32068–32076.

Lin YZ, Yao SY, Veach RA, Torgerson TR, and Hawiger J (1995) Inhibition of nuclear translocation of transcription factor NF-κB by a synthetic peptide containing a cell membrane-permeable motif and nuclear localization sequence. *J Biol Chem* **270:**14255–14258.

McMahon A, Fowler SC, Perney TM, Akemann W, Knopfel T, and Joho RH (2004) Allele-dependent changes of olivocerebellar circuit properties in the absence of the voltage-gated potassium channels Kv3.1 and Kv3.3. *Eur J Neurosci* **19:**3317–3327.

Michaelis ML, Ansar S, Chen Y, Reiff ER, Seyb KI, Himes RH, Audus KL, and Georg GI (2005) β-Amyloid-induced neurodegeneration and protection by structurally diverse microtubule-stabilizing agents. *J Pharmacol Exp Ther* **312:**659–668.

Pan Y, Xu X, Tong X, and Wang X (2004) Messenger RNA and protein expression analysis of voltage-gated potassium channels in the brain of Abeta(25–35)-treated rats. *J Neurosci Res* **77:**94–99.

Pannaccione A, Secondo A, Scorziello A, Calì G, Tagliatatela M, and Annunziato L (2005) NF-kB activation by reactive oxygen species mediates voltage-gated K^+ current enhancement by neurotoxic β-amyloid peptides in NGF-differentiated PC-12 cells and hippocampal neurons. *J Neurochem* **94:**572–586.

Pike CJ, Balazs R, and Cotman CW (1996) Attenuation of beta-amyloid neurotoxicity in vitro by potassium-induced depolarization. *J Neurochem* **67:**1774–1777.

Plant LD, Webster NJ, Boyle JP, Ramsden M, Freir DB, Peers C, and Pearson HA (2006) Amyloid beta peptide as a physiological modulator of neuronal 'A'-type K+ current. *Neurobiol Aging* **27:**1673–1683.

Ramsden M, Plant LD, Webster NJ, Vaughan PF, Henderson Z, and Pearson HA (2001) Differential effects of unaggregated and aggregated amyloid beta protein (1–40) on K^+ channel currents in primary cultures of rat cerebellar granule and cortical neurones. *J Neurochem* **79:**699–712.

Rudy B, Chow A, Lau D, Amarillo Y, Ozaita A, Saganich M, Moreno H, Nadal MS, Hernandez-Pineda R, Hernandez-Cruz A, et al. (1999) Contributions of Kv3 channels to neuronal excitability. *Ann N Y Acad Sci* **868:**304–343.

Rudy B and McBain CJ (2001) Kv3 channels: voltage-gated channels designed for high frequency repetitive firing. *Trends Neurosci* **24:**517–526.

Scorziello A, Pellegrini C, Forte L, Tortiglione A, Gioielli A, Iossa S, Amoroso S, Tufano R, Di Renzo G, and Annunziato L (2001) Differential vulnerability of cortical and cerebellar neurons in primary culture to oxygen glucose deprivation followed by reoxygenation. *J Neurosci Res* **63:**20–26.

Secondo A, Sirabella R, Formisano L, D'Alessio A, Castaldo P, Amoroso S, Ingleton P, Di Renzo G, and Annunziato L (2003) Involvement of PI3′-K, mitogen-activated protein kinase and protein kinase B in the up-regulation of the expression of nNOSalpha and nNOSbeta splicing variants induced by PRL-receptor activation in GH3 cells. *J Neurochem* **84:**1367–1377.

Suh YH and Checler F (2002) Amyloid precursor protein, presenilins, and alpha-synuclein: molecular pathogenesis and pharmacological applications in Alzheimer's disease. *Pharmacol Rev* **54:**469–525.

Tamagno E, Bardini P, Guglielmotto M, Danni O, and Tabaton M (2006) The various aggregation states of beta-amyloid 1–42 mediate different effects on oxidative stress, neurodegeneration, and BACE-1 expression. *Free Radic Biol Med* **41:**202–212.

Tsaur ML, Sheng M, Lowenstein DH, Jan YN, and Jan LY (1992) Differential expression of K+ channel mRNAs in the rat brain and down-regulation in the hippocampus following seizures. *Neuron* **8:**1055–1067.

Yeung SY, Thompson D, Wang Z, Fedida D, and Robertson B (2005) Modulation of Kv3 subfamily potassium currents by the sea anemone toxin BDS: significance for CNS and biophysical studies. *J Neurosci* **25:**8735–8745.

Yu SP (2003) Regulation and critical role of potassium homeostasis in apoptosis. *Prog Neurobiol* **70:**363–386.

Yu SP, Farhangrazi ZS, Ying HS, Yeh CH, and Choi DW (1998) Enhancement of outward potassium current may participate in beta-amyloid peptide-induced cortical neuronal death. *Neurobiol Dis* **5:**81–88.

Yu SP, Yeh C, Strasser U, Tian M, and Choi DW (1999b) NMDA receptor-mediated K^+ efflux and neuronal apoptosis. *Science* **284:**336–339.

Yu SP, Yeh CH, Gottron F, Wang X, Grabb MC, and Choi DW (1999a) Role of the outward delayed rectifier K^+ current in ceramide-induced caspase activation and apoptosis in cultured cortical neurons. *J Neurochem* **73:**933–941.

Yu SP, Yeh CH, Sensi SL, Gwag BJ, Canzoniero LM, Farhangrazi ZS, Ying HS, Tian M, Dugan LL, and Choi DW (1997) Mediation of neuronal apoptosis by enhancement of outward potassium current. *Science* **278:**114–117.

Address correspondence to: Dr. Lucio Annunziato, Division of Pharmacology, Department of Neuroscience, School of Medicine, University of Naples Federico II, Building 19, Via Pansini 5, 80131 Naples, Italy. E-mail: lannunzi@unina.it